



Assessment of SWOT water surface elevations for flood monitoring of a narrow river (< 50 m width)

Amal Mzoughi¹, Mélanie Trudel¹, Pascale Biron², Guénolé Choné², Gabriela L. Siles³

- ¹Department of Civil Engineering and Building Engineering, University of Sherbrooke, 2500, boul. de l'Université, Sherbrooke (Québec) J1K 2R1
- ²Department of Geography, Planning and Environment, Concordia University, 1455 de Maisonneuve Blvd. W., Suite H-1255.26 Montreal (Québec) H3G 1M8
- ³Department of Geomatics, Laval University, 2325 Rue de l'Université, Québec, QC G1V 0A6
- 10 Correspondence to: Amal Mzoughi (amal.mzoughi@usherbrooke.ca)

Abstract. Floods are among the most frequent and damaging natural hazards worldwide, and reliable observations of water surface elevation (WSE) are essential for improving flood modelling and risk management. The Surface Water and Ocean Topography (SWOT) satellite, launched in 2022, offers new opportunities to monitor river hydrodynamics from space, but its performance in relatively narrow rivers (< 50 m width) remains poorly documented. This study evaluates the potential of SWOT WSEs for flood monitoring by comparing them with in situ observations as well as simulations from an existing largescale hydraulic model (LISFLOOD-FP) on the Du Gouffre River (width ≈ 40 m), located in Quebec, Canada. The L2 HR RiverSP (RiverSP) SWOT product Version D, derived from a priori database (SWORD), was first compared with one-minute WSE measurements from a tidal gauge located downstream the Du Gouffre River in the St. Lawrence River. This comparison confirmed the overall quality of the SWOT data in this area, with a root mean square error (RMSE) of 0.24 m. Then, a major flood event (with a return period of about 60 years) which occurred on May 1, 2023, during the SWOT's calibration orbit, was used to conduct a daily analysis of the entire flood event. Eleven observation cycles, covering the period from April 25 to May 7, 2023, were analysed. Limited ground-based observations were available along the studied reach during the flood, highlighting the value of SWOT data. The 1D/2D hydraulic model LISFLOOD-FP was run for the discharges corresponding to eleven SWOT cycles. Overall, there was good agreement with SWOT WSEs, with biases ranging from -0.30 to 0.44 m and RMSEs between 0.14 and 0.54 m. For the peak-flood cycle (May 1), upstream discharges were initially underestimated, and an adjusted LISFLOOD-FP simulation constrained by SWOT observations resulted in a bias of -0.30 m and an RMSE of 0.54 m. This study confirms that SWOT WSEs can provide relevant hydraulic information during flood events in a river below the mission's detection limit, thereby opening the way for a broader use in flood monitoring and modelling.





1 Introduction

40

45

As floods are the most significant and costly natural hazard, efforts are underway around the world to improve how we assess, forecast, and map floods and their impacts (Barendrecht et al., 2017). Hydraulic modelling is the most widely used method for flood mapping to facilitate risk assessment (Teng et al., 2017). A hydraulic model allows the simulation of the spatio-temporal evolution of a river's hydraulic variables such as water surface elevation (WSE) and flow velocity, as well as the flooded area, through the application of mass and momentum conservation equations. It requires information on discharge, boundary conditions of the study domain, and characteristics of the area under study (river shape, roughness). The validation of a hydraulic model mainly depends on the quantity, quality, and type of observed WSE. However, hydraulic models require extensive data, which poses significant challenges (Teng et al., 2017). Given the decline in hydrometric stations (Grimaldi et al., 2016; Mishra and Coulibaly, 2009), their limited spatial and temporal coverage and the limited accessibility of measurement sites, especially during flood periods, observations are not always available or sufficient, which complicates the validation of hydraulic models and affects the reliability of simulations.

In this context, the integration of remotely sensed variables such as WSE (Domeneghetti et al., 2021) and flood extents (Wood et al., 2016) into flood hydraulic modelling could potentially provide valuable information for model validation. Flood extents are usually derived from optical (Huang et al., 2018) or synthetic aperture radar (SAR) sensors (Landuyt et al., 2018). Radar can measure regardless of illumination or weather conditions, whereas optical sensors cannot. This can significantly influence the ability to continuously monitor water, particularly during floods. By overlaying the water extent extracted onto a digital elevation model (DEM), it is possible to retrieve the WSE (Grimaldi et al., 2016), although the accuracy of the WSE value is affected by the resolution of the DEM. Laser and radar altimeters have also been used to measure river WSEs directly (Cretaux et al., 2018). Nielsen et al. (2022) worked with data from several altimetric missions in rivers with widths ranging from a few hundred meters to around 3 km. whereas Li et al. (2023) evaluated how well ICESat-2 laser altimetry could measure WSE in rivers ranging from medium-width (around 1000 m wide) to narrower ones (under 50 m). These findings revealed that, despite advances, getting reliable measurements for rivers narrower than 30 meters and sometimes even those up to 90 meters wide, remains challenging (Li et al., 2023).

The Surface Water and Ocean Topography (SWOT) mission, led by the National Aeronautics and Space Administration (NASA) and the Centre National d'Études Spatiales (CNES), in collaboration with the Canadian Space Agency (CSA) and the UK Space Agency (UKSA), was launched in December 2022 to address these gaps (Biancamaria et al., 2016; Fu et al., 2024). The Ka-band Radar Interferometer (KaRIn), combined with SWOT's low near-nadir incidence angles, enables the satellite to observe at least 90% of the world's rivers wider than 50–100 m, as well as lakes, reservoirs, and wetlands larger than 250 m × 250 m (Biancamaria et al., 2016). The expected vertical accuracy of WSE is 10 cm when pixels are averaged over 1 km² (Peral





et al., 2024). The satellite was initially deployed on a 1-day calibration orbit covering only a certain portion of the Earth between April and July 2023. It was then moved to its nominal 21-day orbit.

To study the potential of the SWOT mission to monitor floods with its 21-day orbit, some studies have been conducted using synthetic SWOT data generated by the CNES large-scale hydrology simulator (SWOT simulator) prior to the mission launch. Frasson et al. (2019) estimated that SWOT would have provided at least one measurement of 55% of the floods recorded between 1985 and 2018 by the Dartmouth Flood Observatory. According to Frasson et al. (2019), SWOT's ability to observe floods mainly depends on the site's latitude and the duration of the event. Indeed, long-duration floods are more likely to be observed more than once. Sites located between 20°S and 20°N will be observed once or twice per 21-day cycle, while higher latitudes will generally be observed two or more times per cycle. Following the satellite's launch, Laipelt et al. (2025) confirm the usefulness of SWOT data for flood studies with a very strong relationship ($R^2 = 0.99$) between actual SWOT observations of WSE variations and in situ measurements during an extreme flood that occurred in southern Brazil in 2024. Such a strong relationship was also obtained between SWOT data and external WSE databases, namely Hydroweb (https://www.theialand.fr/blog/product/hauteur-des-lacs-et-rivieres/) and G-REALM (https://ipad.fas.usda.gov/cropexplorer/global reservoir/) which provide long-term WSE time series for rivers and lakes worldwide. Based on these comparisons, SWOT's global average measurement error is estimated at 0.15 m (Yu et al., 2024). Moreover, SWOT observations also accurately quantified variations in the water surface slope along the studied rivers (Laipelt et al., 2025) and resolved both reach-scale and local variations in WSS and longitudinal profiles (Jiang et al., 2025), with a median RMSE of about 0.25 m for WSE, even in rivers narrower than 100 m (and in some cases < 50 m). Recent large-scale validation over India further demonstrated the strong performance of SWOT WSEs, with over 14,000 observations across 419 stations showing high agreement within situ data, particularly for rivers wider than 100 m with a relative error (RE) of 18 cm, and satisfactory results even for narrower river reaches (RE of 25.78 cm) (Patidar et al., 2025). Nevertheless, studies specifically addressing SWOT performance in narrow rivers remain limited, particularly during a flood event.

This study evaluates the ability of SWOT observations to support the calibration and validation of hydraulic models in a narrow river (Du Gouffre River, Quebec, Canada (≈ 40 m wide)), which experienced a major flood (return period of 60 years, based on three-hour averaged flows (COMEXI-RDG, 2023)) in May 2023, and where a LISFLOOD-FP model (Bates and De Roo, 2000) was available. The Du Gouffre River sector was covered by the SWOT calibration orbit, which made it possible to observe this flood on a daily basis.

2 Methods

2.1 Study Area

The Du Gouffre River (Fig. 1.) is located around 100 km north-east of Quebec City (Quebec, Canada). It is a dynamic meandering river, that crosses the municipalities of Saint-Urbain and Baie-Saint-Paul before joining the St. Lawrence River.



100



The floodplain is between 300 and 400 m wide, with an average active channel width of about 40 m. The upstream sector of Saint-Urbain is characterized by a slope of 0.30%, which decreases to 0.11% in the sector of Baie-Saint-Paul. The downstream parts of the Du Gouffre River valley are influenced by the tides of the St. Lawrence River. The watershed of the Du Gouffre River covers an area of about 991 km². Among the main tributaries, the Bras du Nord Ouest River (100 km²) and the Des Mares River (115 km²) also represent important sub-watersheds within the Du Gouffre watershed (Fig. 1.). The region is subject to frequent flooding (Gouvernement du Québec, 2023), especially in the Baie-Saint-Paul area, where the Du Gouffre River and the Bras du Nord-Ouest River meet within an urban perimeter. Three types of flooding can occur on the Du Gouffre River: open water flooding caused by heavy rainfall or snowmelt, ice jam flooding, and flooding caused by the overflow of the St. Lawrence River along the Baie-Saint-Paul shoreline during high tides and strong winds.

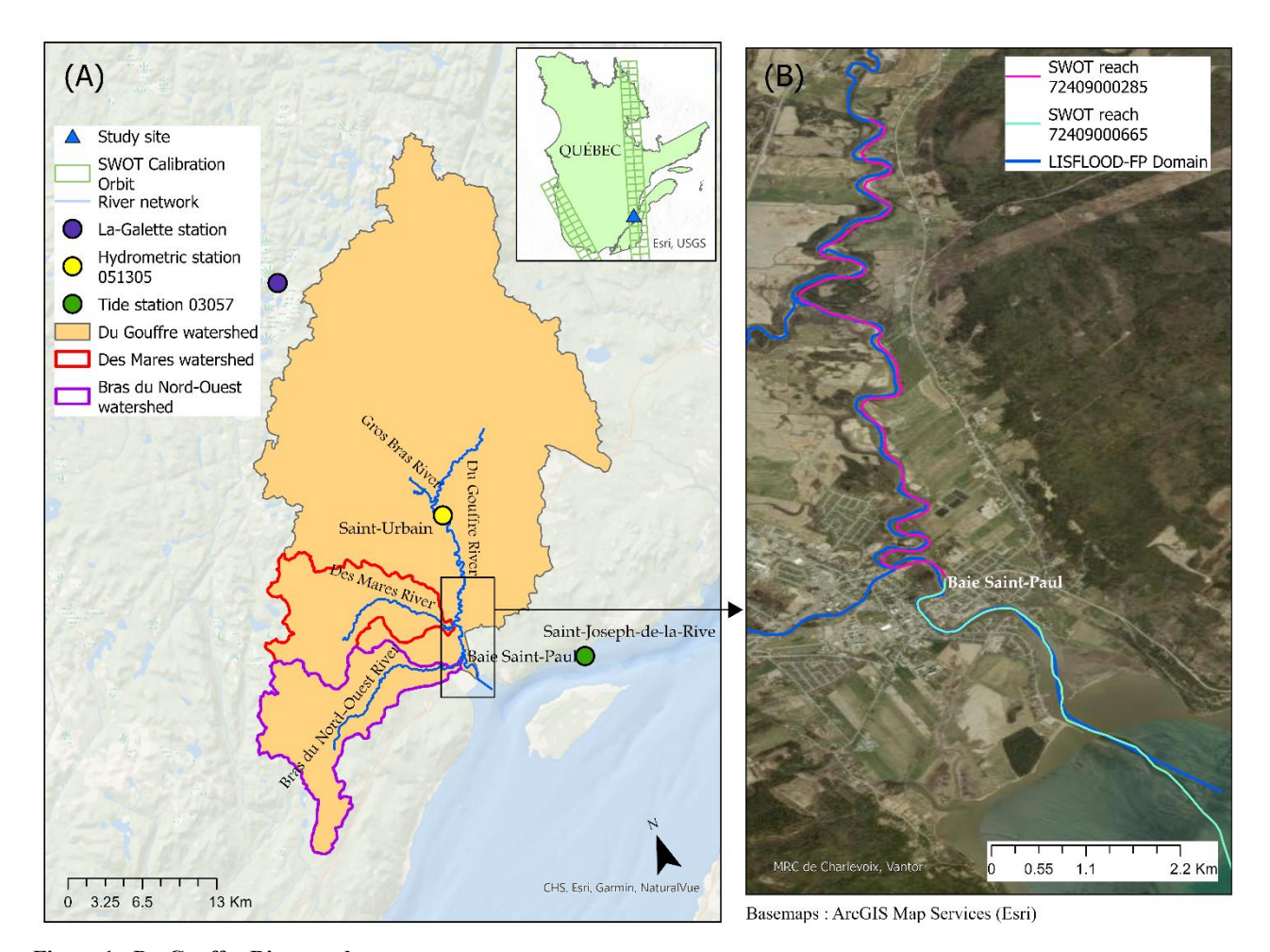


Figure 1: Du Gouffre River study area



105

110

115

120



2.2 Flood Event

On May 1, 2023, an exceptional flood occurred in the Du Gouffre watershed. It was preceded by two weeks of spring snowmelt, during which approximately 170 mm of water from the snowpack flowed into the basin. This situation was exacerbated by the heavy rainfall between April 30 and May 2, 2023, totalling 95 mm at the centre of the watershed at Saint-Urbain, with up to 142 mm of rain recorded at the La-Galette station, located at the head of the watershed (Fig. 1.), including almost 100 mm in the space of just 12 hours (Gouvernement du Québec, 2023). These rainfall amounts, far exceeding the monthly averages for May (around 81 mm at La-Galette and 88 mm at Saint-Urbain), were intensified by a strong orographic effect in the high-altitude areas (Gouvernement du Québec, 2023). The river flow thus increased from 75 m³/s to 500 m³/s in the span of 12 hours, peaking around 12:30 p.m. (local time: UTC-4) on May 1 (Fig. 2.). The recurrence of this flood at the hydrometric station 051305 (Station 051305, 2025) in Saint-Urbain corresponds to a return period of 60 years for the maximum three-hour discharge, and 150 years for the daily average discharge. In the lower part of the river, near Baie-Saint-Paul, tidal fluctuations can also influence WSE and may contribute to worsening flood conditions when coinciding with river discharge peak. The SWOT satellite captured the May 1 flood through 13 acquisitions made before, during, and after the event (Fig. 2.). For this study, the comparison with SWOT observations focuses on the period from April 25 to May 7, 2023, excluding cycles 504 and 505 due to invalid data.

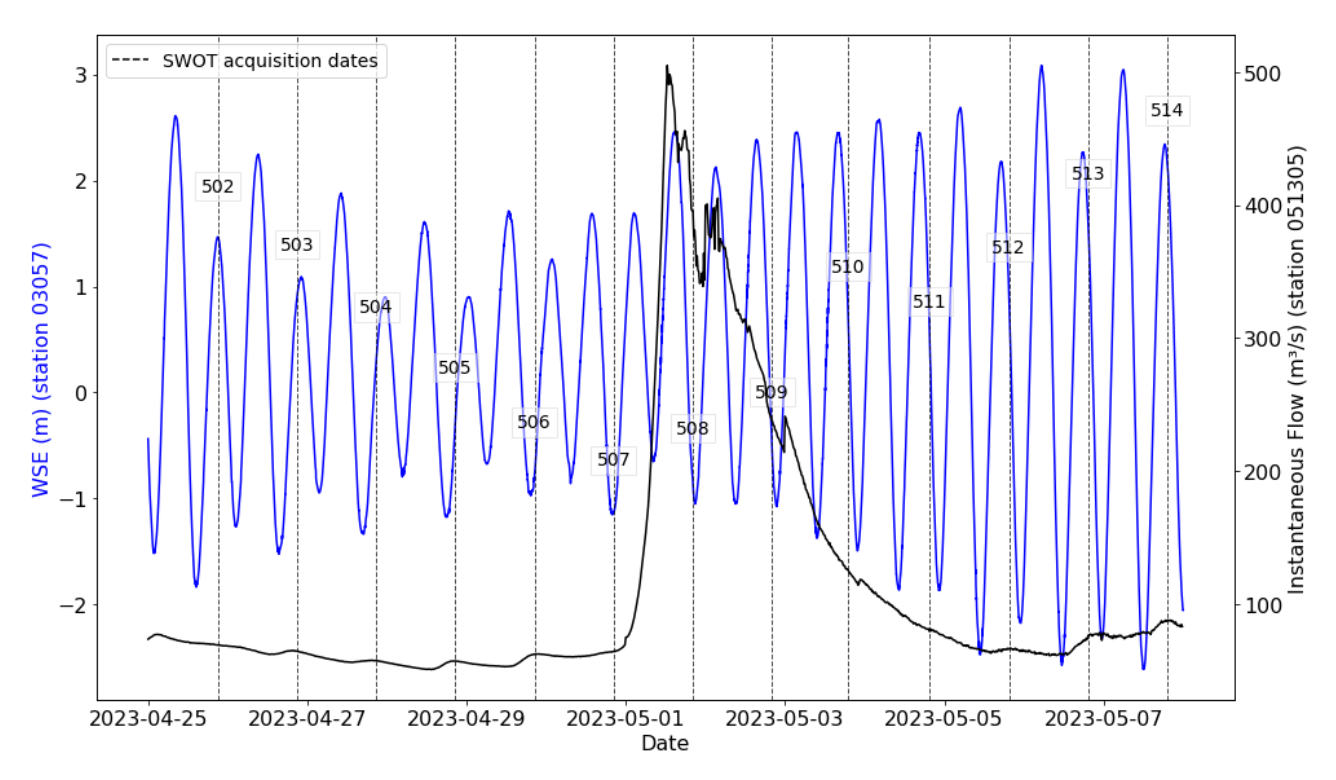


Figure 2: Instantaneous discharge (black curve) measured at hydrometric station 051305, and the WSE (blue curve) recorded at the tide gauge station 03057 (Station 03057, 2025), from April 25 to May 7, 2023. The black dots indicate the dates of SWOT satellite



125

130

135

140

150



acquisitions during its calibration orbit. The peak of the flood (reaching nearly 500 m³/s) occurred on May 1, 2023, at 12:30 p.m. (Local Time).

2.3 Hydraulic Modelling: LISFLOOD-FP

An existing LISFLOOD-FP 1D-2D hydraulic model was used to simulate WSE and flooded areas in the Du Gouffre River between Saint-Urbain and Baie-Saint-Paul. This model, described in Choné et al. (Choné et al., 2021, 2024), had been applied prior to the 2023 flood in this area as part of a large-scale modelling project based on high-resolution LiDAR (Light Detection And Ranging) data.

Unlike conventional hydraulic models such as HEC-RAS, which are typically site-specific, strongly calibrated, and reliant on extensive in situ datasets, LISFLOOD-FP was explicitly designed for large-scale floodplain applications where such detailed data are often unavailable. It employs a simplified raster-based framework with an estimated, thereby reducing both computational costs and input data requirements (Bessar et al., 2021; Horritt and Bates, 2001; Moghim et al., 2023). It uses an approach that solves the Saint-Venant equations on a 2D grid corresponding to the provided DEM for overbank flow and a 1D representation of in-channel flow, neglecting the advection term in the momentum equation, following the simplified approach proposed by Bates et al. (2010). The model is fed solely by remote-sensed data, incorporating an inverse hydraulic model to estimate bed elevation from LiDAR water surfaces, using the known discharge value on the LiDAR day of acquisition (Choné et al., 2021, 2024). The hydraulic model is not calibrated, using a constant Manning's n over the studied area.

Model boundary conditions include instantaneous discharge series applied at several domain entry points, as well as downstream WSEs provided by the tidal gauging station ((Station 03057, 2025), Fig. 2.). Tide data were initially provided at map datum (ZC), then corrected by -3.311 m to convert them to the Canadian Geodetic Vertical Datum of 1928 (CGVD28, epoch 1997) to ensure consistency of WSEs with the rest of the data used in the modelling.

The May 2023 flood modified the geomorphology of the Du Gouffre River and altered the historical relationships between WSE and discharge at the Saint-Urbain hydrometric station (Station 051305, 2025). To take these changes into account, a new rating curve was developed by using the Baratinage software (INRAE, 2023), based on the available observations and their associated uncertainties. By interpolating the relationships between WSE and discharge, we were able to associate each WSE value with an average, a minimum and a maximum discharge. Since the Saint-Urbain station is located 11.6 km upstream of the SWOT study area, a drainage area transfer was applied across the LISFLOOD domain to account for spatial differences. The drainage area at Saint-Urbain is 632 km², compared with 889 km² at Baie-Saint-Paul, and this scaling was used consistently to derive discharges at all input points of the model, therefore assuming a constant specific discharge.

Unlike the other cycles, during the peak flood of May 1 (cycle 508), the drainage-area-based transfer applied across the LISFLOOD-FP domain was not sufficient to capture the actual hydraulic conditions. The transposed discharge at the Saint-Urbain station (357 m³/s) was lower than the maximum value of 505 m³/s recorded only a few hours before the SWOT overpass (Fig. 2). Given the 11.6 km distance between the station and the upstream limit of the SWOT-observed reach, it is plausible that the true discharge was higher at the time of acquisition. Furthermore, tributaries originating from the Nord-Ouest Massif,



160



particularly the Des Mares River, contributed significant additional inflows during the event. The transposed discharge for this tributary was 82 m³/s, whereas Marquis et al. (2024) suggests that actual peak flows may have ranged between 150 and 200 155 m³/s. Radar-based analyses suggest that rainfall over the Nord-Ouest Massif was significantly more intense than recorded at available stations, potentially exceeding 240 mm according to Marquis et al. (2024), which further supports the hypothesis of underestimated discharges. Consequently, a specific discharge adjustment was performed for the Des Mares tributary, with tested inflows up to 240 m³/s, while the main channel discharge was constrained by the maximum value observed at Saint-Urbain (505 m³/s). This calibration, supported by SWOT observations, provided a more realistic hydraulic representation of the flood conditions for cycle 508 than that solely based on a drainage area ratio from the St-Urbain gauging station. Table 1 summarizes the discharges derived from the rating curve of the Saint-Urbain gauging station (Station 051305, 2025) for each SWOT overpass. These discharges served as the reference for drainage-area transposition across the LISFLOOD-FP domain. Downstream WSE correspond to observations at the Saint-Joseph station (Station 03057, 2025).

Following Choné et al., (Choné et al., 2021, 2024), a constant Manning's roughness coefficient (n) of 0.03 was applied to the 165 channel, whereas the Manning's n in the floodplain was based on land-use data following Chow (1959).

Table 1: Discharges derived from the Saint-Urbain rating curve during SWOT overpasses, used in LISFLOOD-FP (prior to discharge calibration for cycle 508).

Date	SWOT Cycle	SWOT Overpass (UTC-4)	Q Mean (m3/s)	Q Min (m3/s)	Q Max (m3/s)	WSE station 03057 (m)
04/25/2023	502	21:06	78	68	87	1.47
04/26/2023	503	20:57	70	62	78	0.93
04/29/2023	506	20:30	70	63	78	-0.77
04/30/2023	507	20:21	73	65	81	-1.12
05/01/2023	508	20:10	357	287	444	-0.88
05/02/2023	509	20:01	197	164	237	-0.47
05/03/2023	510	19:51	101	88	116	0.00
05/04/2023	511	19:42	78	68	87	0.33
05/05/2023	512	19:32	63	57	69	0.92
05/06/2023	513	19:24	73	65	81	1.58
05/07/2023	514	19:14	78	68	87	2.17



175

180

185

190

195

200



170 2.4 SWOT data analysis

The SWOT River data processing chain begins with the L2_HR_PIXC product (PIXC), a pixel cloud in NetCDF format containing, among other attributes, ellipsoidal heights, geographic coordinates, surface classification (water, near-water, near-land, and land), pixel area, and quality flags. The RiverObs algorithm developed by Ernesto Rodriguez, available at GitHub (https://github.com/SWOTAlgorithms/RiverObs) then takes the PIXC product as input, along with the SWORD (Surface Water and Ocean Topography River Database), which structures rivers into segments (reaches) of about 10 km, themselves subdivided into nodes spaced approximately 200 m apart (Altenau et al., 2021). As a first step, RiverObs generates the L2_HR_PIXCVEC product (PIXCVEC), which filters and vectorizes valid water pixels to reduce noise and improve geometric accuracy and ensure proper geolocation. Using PIXCVEC and the SWORD river geometry, RiverObs produces the final L2_HR_RiverSP product (RiverSP), in which water pixels are associated with their nearest node or reach, and hydrological attributes are aggregated accordingly (Stuurman et al., 2023).

The RiverSP (Single-Pass) product is distributed in shapefile format, with separate files for reaches (line features) and nodes (point features). These include aggregated attributes such as WSE, surface width, water surface area, as well as quality flags associated with each node. Estimated discharge (not available at the time of this study) and slope are provided at the reach level only. In this study, only the WSE values from the node product are used, with the aim of comparing them to the WSEs simulated by the LISFLOOD-FP hydraulic model. In SWOT products, WSE refers to the elevation of the inland water surface relative to the geoid, after removing tide effects (Chen et al., 2025). Version D (PGD0) of the SWOT RiverSP product, which includes the wse_sm attribute, was used in this study, as this smoothed variable reduces noise and ensures better spatial continuity between nodes, making it more suitable for hydraulic comparisons (Stuurman et al., 2025).

SWOT node data were filtered to eliminate unreliable observations. Two quality flag fields were used: node_q and xovr_cal_q. The node_q field, is a summary quality indicator for the node, derived from the aggregation of PIXC product pixels assigned to the corresponding node, indicates the overall quality of the observation at the node level and can take the following values: 0 (good), 1 (suspect), 2 (degraded), and 3 (bad). In parallel, the xovr_cal_q flag was selected because it is the only indicator that specifically assesses the reliability of the cross-over calibration (see Peral et al., 2024 for details on the cross-over calibration). It takes three values: 0 (nominal measurement), 1 (suspect measurement), and 2 (bad measurement). Only nodes with a node_q value less than or equal to 2 and a xovr_cal_q value equal to 0 or 1 were retained to limit the influence of points with known anomalies. The other quality flags should be the subject of further investigation before being used for data filtering. In addition, some nodes were removed manually despite satisfying both quality criteria, as their WSE values were clearly inconsistent with the river's typical elevation range and deviated significantly from adjacent node values.

The WSEs provided in the SWOT product are expressed in the ITRF2014 reference frame, based on the WGS84 ellipsoid and associated with the EGM2008 geoid. The adopted ITRF realization is referenced to the epoch of the measurements (Chen et al., 2025). To ensure compatibility with the WSEs simulated by the LISFLOOD-FP model, all SWOT observations were converted to the Canadian Spatial Reference System (CSRS). In this study the NAD83 (CSRS) reference frame (epoch 1997.0)

https://doi.org/10.5194/egusphere-2025-5449 Preprint. Discussion started: 25 November 2025

© Author(s) 2025. CC BY 4.0 License.



205

210

215

220

225



and the CGVD28 vertical datum were used. The conversion was performed using the TRX and GPS-H tools provided by Natural Resources Canada (https://ressources-naturelles.canada.ca/carte-outils-publications/donnees). This step aimed to place all data in a common reference frame, to make SWOT observations directly comparable to the results simulated by the hydraulic model.

For each SWOT node retained after filtering, the corresponding WSE simulated by the LISFLOOD-FP model was extracted from the WSE raster. When the node did not coincide exactly with a valid raster cell, the value of the nearest cell was used. This method ensured full spatial correspondence between SWOT observations and the model results over the entire study period. To compare WSE from SWOT observations and hydraulic modelling, two statistical indicators were calculated for each overpass date: the root mean square error (RMSE), which measures the overall difference between the values produced by the LISFLOOD-FP hydraulic model and those measured by the SWOT satellite, and the bias, which highlights any systematic trends of overestimation or underestimation. The SWOT mission requirements are expressed using the 1-sigma metric, which is the 68th percentile of the absolute error between SWOT and the observations. This metric is therefore used to compare WSE SWOTs with observations at stations.

3 Results

The extracted WSEs from SWOT products (PGD0) were first compared with measurements (at one-minute intervals) from tide gauge station 03057 (Saint-Joseph-de-la-Rive, Fig. 1A) for all satellite passes between April 2023 and August 2025, during ice-free period. Figure 4 shows the probability that the absolute WSE error is less than or equal to a given value, indicating that the 68th percentile (corresponding to the 1-sigma metric defined in the SWOT requirements) is 0.05 m, with an RMSE of 0.24 m. The SWOT observations used are of good quality (node $_q < 3$ et xovr $_cal_q < 2$). The obtained values meet the accuracy thresholds defined by the SWOT mission, which corresponds to the expected accuracy of 0.10 m averaged over 1 km² or 0.45 m averaged over 0.01 km² (Desai, 2018).

The consistency of the SWOT WSEs with LISFLOOD-FP simulations was assessed by comparing the corresponding nodes, which represents the core of this study. SWOT observations were thus compared with the results of the LISFLOOD-FP hydraulic model for seven observation cycles between April 25 and May 7, 2023 (Table 2). The differences between the two sources remain relatively small, with bias values ranging from -0.30 to 0.44 m and RMSE values between 0.27 and 0.54 m, indicating good agreement between SWOT observations and LISFLOOD-FP simulations. Detailed bias and RMSE values are shown in Table 2.





Table 2. Comparison of WSEs observed by SWOT with the results of the LISFLOOD-FP model, for each SWOT cycle (Cycles 504-505 lack valid data; Cycle 510 excluded after filtering).

SWOT cycle	Bias (m)	RMSE (m)
502	0.44	0.52
503	0.43	0.47
506	0.33	0.50
507	0.28	0.47
508	-0.30	0.54
509	-0.07	0.14
510	-	-
511	0.24	0.40
512	0.03	0.33
513	0.33	0.40
514	0.18	0.29

The observed flood is covered by cycles 508, 509, and 510. For cycle 508, which corresponds to the flood peak reached on May 1, a discharge calibration was carried out for the Des Mares tributary using SWOT-derived WSEs. Increasing the tributary inflow to 240 m³/s yielded a bias of -0.30 m and an RMSE of 0.54 m (Fig. 3.), demonstrating that SWOT effectively helps calibrate discharge estimates when they are poorly known. For this figure, no discharge uncertainty is considered, as the value of 240 m³/s corresponds to the calibrated flow used in the simulation.





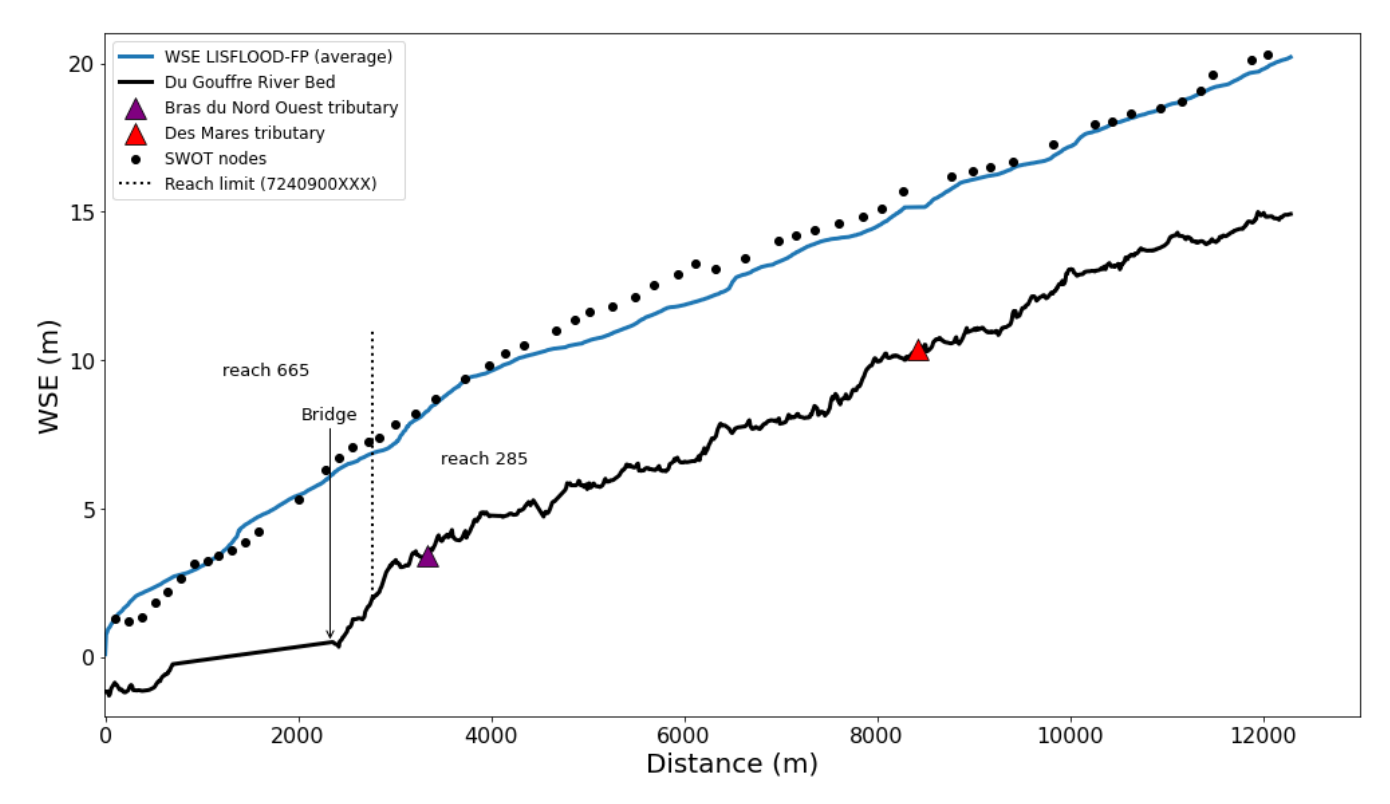


Figure 3: Comparison of SWOT and LISFLOOD-FP WSEs during the flood peak (cycle 508, May 1, 2023)

The following cycle, 509, shows a good agreement between the two sources. The SWOT points generally align well with the simulated WSEs (Fig. 4.). The bias is -0.07 m and the RMSE is 0.14 m. Unlike cycle 508, the discharges for this overpass were well constrained and did not involve significant tributary inputs, which likely contributed to the strong consistency between the two datasets.

SWOT data corresponding to cycle 510 could not be used. In this case, all nodes were associated with a xovr_cal_q value equal to 2, indicating a cross-over calibration that was considered unreliable. By applying the quality filters defined above, all these observations were discarded.

Cycles 502, 503, 506 and 507 precede the flood peak. The discrepancies between SWOT and the model are slightly more pronounced than those observed during the recession phase. Biases range from 0.28 m to 0.44 m, and RMSEs from 0.47 m to 0.52 m. During the recession phase, covered by cycles 511, 512, 513 and 514, the discrepancies are smaller; the biases do not exceed 0.33 m and the RMSE values range are from 0.29 m to 0.40 m.

245

250





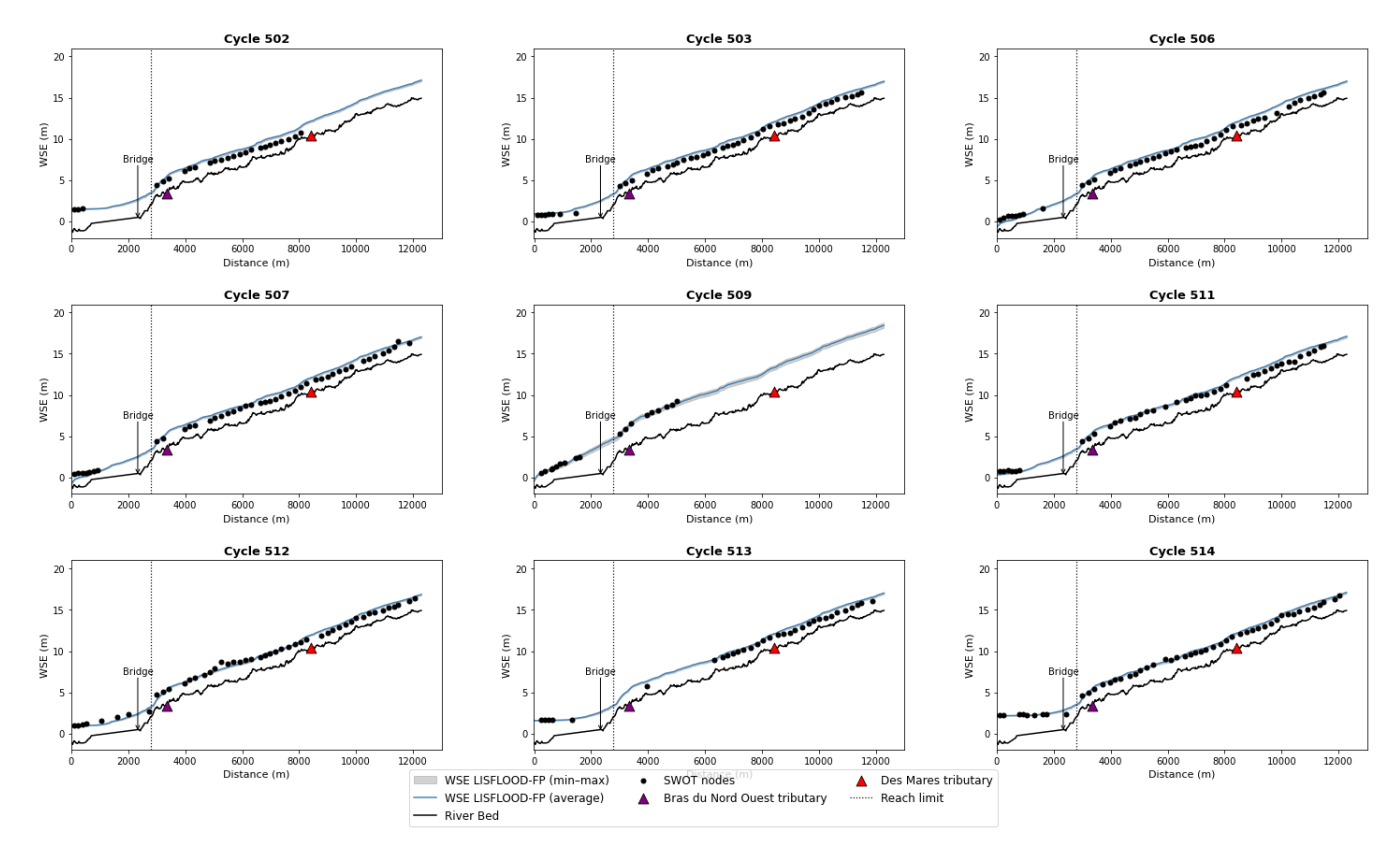


Figure 4: Comparison of SWOT and LISFLOOD-FP WSEs for all cycles before and after the May 1 flood (excluding Cycle 508); the maximum and minimum discharges based on the uncertainty of the rating curve are also represented.

4 Discussion and Conclusion

275

The results obtained show a general consistency between the SWOT observations and the WSEs simulated by the LISFLOOD-FP model over most of the cycles studied. The RMSE values ranging from 0.14 m to 0.54 m and biases values between -0.30 and 0.44 m. These results are for river reaches of about 40 m in width, which is significantly smaller than rivers studied using simulated and actual SWOT data (e.g., 100–500 m, Domeneghetti et al., 2018; >300 m, Nair et al., 2022; 5.4 to 490 km, Yu et al., 2024; ~10 km, Laipelt et al., 2025). According to Domeneghetti et al. (2018), the narrower the river, the lower the performance of SWOT.

In this study, the discrepancies between the SWOT observations and the hydraulic simulations remain at a level of precision that is sufficient to support the calibration and validation of hydraulic models. These results suggest that SWOT observations can offer satisfactory accuracy even in the context of narrow rivers, thereby helping to broaden their range of application. Some studies indicate that vertical errors on the order of a few tens of centimeters can be sufficient to calibrate hydraulic models. For example, Shen et al. (2020) used altimetric observations from the Sentinel-3A and CryoSat-2 satellites to calibrate a one-dimensional model of the Han River in China. While initial RMSE values reached 0.22 m and 0.49 m respectively, the calibration brought them down to between 0.10 m and 0.22 m. The authors concluded that altimetric data with RMSEs below



280

285

305

310



0.6 m can be considered accurate enough to make a meaningful contribution to improving hydraulic simulations. On the Po River, Schneider et al. (2018) demonstrated the added value of continuous CryoSat-2 observations (average RMSE of 0.38 m), which were used to refine the spatial distribution of roughness coefficients in a hydraulic model. The results were comparable to those obtained using traditional gauging methods. Also on the Po River, Domeneghetti et al. (2014) pointed out that, although ERS-2 and ENVISAT altimetric data had relatively high RMSE (0.73–0.85 m), their combined use improved the depiction of the hydrological regime and the slope of the water profile when included in a joint calibration alongside ground-based measurements. More recently, Coppo Frias et al. (2023) showed that it was possible to model rivers less than 100 m wide using a simplified hydraulic model and ICESat-2 products, achieving validation RMSEs between 0.41 m and 0.44 m. Lastly, Zhou et al. (2023) used a combination of ICESat-2 and Sentinel-2 data in the Yiluo River basin to estimate WSEs with RMSE ranging from 0.25 m to 0.59 m. The model calibrated with these data then achieved a validation RMSE of 0.36 m, further supporting the idea that this level of precision is more than sufficient for simulating WSE and floods, even in poorly gauged catchments.

In cycle 508 (May 1 flood peak), calibrating the Des Mares tributary inflow with SWOT-derived WSEs greatly improved the hydraulic model's performance, yielding a bias of -0.30 m and an RMSE of 0.54 m. This result demonstrates that SWOT observations can reveal discharge underestimation in ungauged tributaries and can effectively calibrate model inputs and reduce uncertainty. Similar findings were reported by Diouf et al. (2025), who demonstrated that SWOT's centimeter-level accuracy can substantially enhance model calibration in poorly instrumented environments, particularly by constraining hydraulic parameters and improving the representation of WSE dynamics in zones lacking in situ measurements. At the same time, the need for such adjustment underscores the inherent challenge of determining an accurate discharge representation in hydraulic models under conditions of spatial rainfall variability. Spatial variability in rainfall strongly influences flood runoff, they can alter the volume, timing, and peak flow of the hydrograph (Khakbaz et al., 2012). Discharge estimates that may become available in future versions of SWOT products (and already for some reaches in version D) will be particularly valuable in such situations, as they could help refine the discharge inputs used in hydraulic models.

Additional validation elements confirm the reliability of SWOT observations during the flood peak. Drone imagery acquired on May 1 (cycle 508) (Appendix A, Fig. A1) illustrates the extent of the flooding observed in the field. The extent of the flooded areas visible in these images is consistent with the WSEs measured by the satellite, thus providing an independent validation for the SWOT observations.

This agreement is further supported by the analysis of two internal quality indicators provided in the SWOT River SP product (Fig. 5). The first, wse_u, represents the total uncertainty (random and systematic) of the WSE at each node (in meters), while the second, dark_frac, corresponds to the fraction of "dark water" pixels used in the retrieval, expressed as a unitless ratio between 0 and 1. Dark water results from signal attenuation, which can be caused by rainfall or by a smooth water surface (e.g., in the absence of wind). This raises the question of whether dark water occurs more frequently during flood events. For cycle 508, most wse_u values are tightly clustered between 0.09 m and 0.24 m, with a median around 0.13 m, indicating a generally low total uncertainty for most nodes. Only a few outliers exceed 0.3 m, reaching up to 0.76 m, but these remain

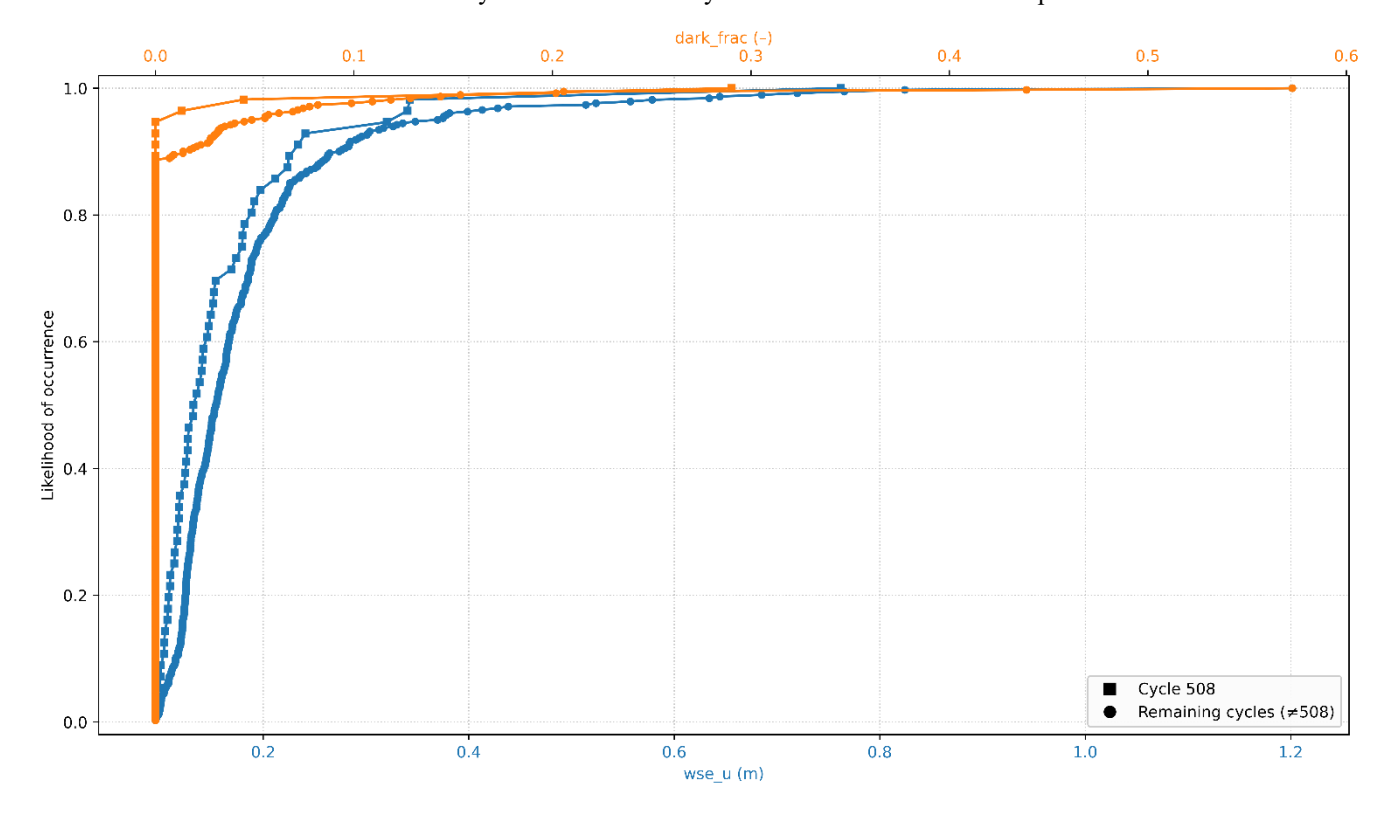


315

325



exceptions. Regarding dark_frac, almost all nodes have values equal to 0, with only three points above zero (\leq 0.3 m). When compared with the remaining cycles (Fig. 5.), the distribution of wse_u values is similarly concentrated, with a median of 0.15 m. Similarly, dark_frac, values remain consistently close to 0 for all cycles, confirming the robustness of water detection throughout the study period. Taken together, these indicators show that the SWOT observations during the flood peak were of sufficient quality to ensure reliable WSE estimates. This case study demonstrates that the combination of SWOT observations with LISFLOOD-FP modelling provides valuable insights into discharge dynamics in poorly gauged reaches, particularly under extreme flood events where tributary contributions and hydraulic uncertainties are most pronounced.



320 Figure 5: Cumulative distribution of SWOT quality indicators (wse u in meters, dark frac unitless) across cycles.

During cycle 509, which corresponds to the recession phase, SWOT observations and model hydraulic simulations show limited deviations. The bias remains low (-0.07 m) and the RMSE is 0.14 m, showing a high degree of consistency between the two datasets.

Cycle 510 was excluded from the analysis because all available observations had an xovr_cal_q value of 2, indicating low-quality cross-calibration. This shows the value of using the quality indicators supplied with the data to assess their reliability prior to any comparison with a model. The use of enhanced reprocessed products should improve the accuracy and reliability of WSEs. The implementation of an automatic filter based on these indicators would represent a relevant approach to simplify the identification of usable data.





The pre- and post-flood cycles (503-507, and 511-514), as well as cycle 509 in the recession phase, show good agreement between the WSEs observed by SWOT and those simulated by the LISFLOOD-FP model. RMSEs are between 0.14 m and 0.52 m. Such results also suggest that, in cases of systematic discrepancies, SWOT observations could be used as a basis for calibrating large-scale hydraulic models. These findings are in line with the conclusions of Frasson et al (2019), according to which SWOT data, despite their irregular spatio-temporal nature, can be useful for evaluating or adjusting hydraulic models, particularly when acquired after a flood event.

335

340

345





Appendix A



Fig. A1 Aerial photograph showing the extent of flooding along the Du Gouffre River in Baie-Saint-Paul, on May 1, 2023, at 18:59 (photograph courtesy of Frederick Tremblay, via Facebook).

360

355

https://doi.org/10.5194/egusphere-2025-5449 Preprint. Discussion started: 25 November 2025

© Author(s) 2025. CC BY 4.0 License.



EGUsphere Preprint repository

Code and data availability

The SWOT RiverSP products used in this study are freely available from the NASA Earthdata portal at https://www.earthdata.nasa.gov/. Hydrometric data were obtained from the Centre d'expertise hydrique du Québec (CEHQ), and tidal observations at the Saint-Joseph station were provided by the Canadian Hydrographic Service. The LISFLOOD-FP hydraulic model was used for the simulations, and the processing scripts used in this study are available upon reasonable

request from the corresponding author.

Author contributions

AM: designed the study, processed the SWOT and LISFLOOD-FP data, conducted the analyses, and led the writing of the manuscript. MT: supervised all aspects of the study, including the SWOT data analysis, hydraulic modelling, and manuscript preparation, and provided expert guidance in remote sensing. PB: co-supervised the study, contributed to the hydraulic modelling and data interpretation, and participated in manuscript revisions. GC: supported the LISFLOOD-FP model implementation and contributed to the processing and analysis of simulation results. GLS: provided expertise on SWOT data processing and analysis and helped with geodetic conversions. All authors reviewed and approved the final version of the

manuscript.

The authors declare that they have no conflict of interest.

Acknowledgments

Parts of the manuscript were translated from French to English using the DeepL translator. In addition, artificial intelligence tools (e.g. ChatGPT, OpenAI) were used to support the correction of Python code. The scientific content, analysis, and interpretation remain entirely the responsibility of the authors.

Financial support

This research was supported by the Canadian Space Agency under grant no. 24AO3SHE16.

390

395





References

- Altenau, E. H., Pavelsky, T. M., Durand, M. T., Yang, X., Frasson, R. P. D. M., and Bendezu, L.: The Surface Water and Ocean Topography (SWOT) Mission River Database (SWORD): A Global River Network for Satellite Data Products, Water Resour. Res., 57, e2021WR030054, https://doi.org/10.1029/2021WR030054, 2021.
 - Barendrecht, M. H., Viglione, A., and Blöschl, G.: A dynamic framework for flood risk, Water Secur., 1, 3-11, 2017.
 - Bates, P. D., Horritt, M. S., and Fewtrell, T. J.: A simple inertial formulation of the shallow water equations for efficient two-dimensional flood inundation modelling, J. Hydrol., 387, 33–45, 2010.
- Bessar, M. A., Choné, G., Lavoie, A., Buffin-Bélanger, T., Biron, P. M., Matte, P., and Anctil, F.: Comparative analysis of local and large-scale approaches to floodplain mapping: a case study of the Chaudière River, Can. Water Resour. J. Rev. Can. Ressour. Hydr., 46, 194–206, https://doi.org/10.1080/07011784.2021.1961610, 2021.
 - Biancamaria, S., Lettenmaier, D. P., and Pavelsky, T. M.: The SWOT Mission and Its Capabilities for Land Hydrology, in: Remote Sensing and Water Resources, vol. 55, edited by: Cazenave, A., Champollion, N., Benveniste, J., and Chen, J., Springer International Publishing, Cham, 117–147, https://doi.org/10.1007/978-3-319-32449-4 6, 2016.
- Chen, C., Moller, D., Rodriguez, E., and Esteban-Fernandez, D.: SWOT Science Data Products User Handbook, NASA Jet Propulsion Laboratory (JPL), California Institute of Technology, Pasadena, California, 2025.
 - Choné, G., Biron, P. M., Buffin-Bélanger, T., Mazgareanu, I., Neal, J. C., and Sampson, C. C.: An assessment of LARGE-SCALE flood modelling based on LIDAR data, Hydrol. Process., 35, e14333, https://doi.org/10.1002/hyp.14333, 2021.
- Choné, G., Biron, P., and Buffin-Bélanger, T.: Vers une cartographie générale des zones inondables Phase 3 Évaluation des incertitudes associées à la modélisation hydraulique appliquée à large échelle pour des cours d'eau du Québec habité, Ministère de l'Environnement, de la Lutte contre les changements climatiques, de la Faune et des Parcs (MELCCFP), Québec, Canada, 2024.
 - Chow, V. T.: Determination of Hydrologic Frequency Factor, J. Hydraul. Div., 85, 93–98, https://doi.org/10.1061/JYCEAJ.0000327, 1959.
- 420 Coppo Frias, M., Liu, S., Mo, X., Nielsen, K., Ranndal, H., Jiang, L., Ma, J., and Bauer-Gottwein, P.: River hydraulic modeling with ICESat-2 land and water surface elevation, Hydrol. Earth Syst. Sci., 27, 1011–1032, 2023.
 - Cretaux, J.-F., Berge-Nguyen, M., Calmant, S., Jamangulova, N., Satylkanov, R., Lyard, F., Perosanz, F., Verron, J., Samine Montazem, A., and Le Guilcher, G.: Absolute calibration or validation of the altimeters on the Sentinel-3A and the Jason-3 over Lake Issykkul (Kyrgyzstan), Remote Sens., 10, 1679, 2018.
- Diouf, A., Salameh, E., Sakho, I., Sow, B. A., Deloffre, J., López Solano, C., Turki, E. I., and Lafite, R.: Use of SWOT Data for Hydrodynamic Modelling in a Tropical Microtidal Estuarine System: The Case of Casamance (Senegal), Remote Sens., 17, 3252, 2025.
 - Domeneghetti, A., Tarpanelli, A., Brocca, L., Barbetta, S., Moramarco, T., Castellarin, A., and Brath, A.: The use of remote sensing-derived water surface data for hydraulic model calibration, Remote Sens. Environ., 149, 130–141, 2014.
- Domeneghetti, A., Schumann, G.-P., Frasson, R. P. M., Wei, R., Pavelsky, T. M., Castellarin, A., Brath, A., and Durand, M. T.: Characterizing water surface elevation under different flow conditions for the upcoming SWOT mission, J. Hydrol., 561, 848–861, 2018.





- Domeneghetti, A., Molari, G., Tourian, M. J., Tarpanelli, A., Behnia, S., Moramarco, T., Sneeuw, N., and Brath, A.: Testing the use of single-and multi-mission satellite altimetry for the calibration of hydraulic models, Adv. Water Resour., 151, 103887, 2021.
 - Frasson, R. P. D. M., Schumann, G. J. -P., Kettner, A. J., Brakenridge, G. R., and Krajewski, W. F.: Will the Surface Water and Ocean Topography (SWOT) Satellite Mission Observe Floods?, Geophys. Res. Lett., 46, 10435–10445, https://doi.org/10.1029/2019GL084686, 2019.
- Fu, L., Pavelsky, T., Cretaux, J., Morrow, R., Farrar, J. T., Vaze, P., Sengenes, P., Vinogradova-Shiffer, N., Sylvestre-Baron, A., Picot, N., and Dibarboure, G.: The Surface Water and Ocean Topography Mission: A Breakthrough in Radar Remote Sensing of the Ocean and Land Surface Water, Geophys. Res. Lett., 51, e2023GL107652, https://doi.org/10.1029/2023GL107652, 2024.
 - Gouvernement du Québec, M. des A. municipales et de l'Habitation: Inondation causée par la rivière du Gouffre le 1er mai 2023 : portrait des aléas en cause, Gouvernement du Québec, Québec, Canada, 2023.
- Grimaldi, S., Li, Y., Pauwels, V. R. N., and Walker, J. P.: Remote Sensing-Derived Water Extent and Level to Constrain Hydraulic Flood Forecasting Models: Opportunities and Challenges, Surv. Geophys., 37, 977–1034, https://doi.org/10.1007/s10712-016-9378-y, 2016.
 - Horritt, M. S. and Bates, P. D.: Predicting floodplain inundation: raster-based modelling versus the finite-element approach, Hydrol. Process., 15, 825–842, https://doi.org/10.1002/hyp.188, 2001.
- Huang, C., Chen, Y., Zhang, S., and Wu, J.: Detecting, Extracting, and Monitoring Surface Water From Space Using Optical Sensors: A Review, Rev. Geophys., 56, 333–360, https://doi.org/10.1029/2018RG000598, 2018.
 - INRAE: BaRatinAGE v3 Logiciel pour courbes de tarage et estimation d'incertitude, 2023.
 - Jiang, L., Nielsen, K., Andersen, O. B., and Liu, J.: SWOT Reveals Detailed Dynamics of Longitudinal River Slope in the Missouri River Basin, Geophys. Res. Lett., 52, e2025GL115953, https://doi.org/10.1029/2025GL115953, 2025.
- Khakbaz, B., Imam, B., Hsu, K., and Sorooshian, S.: From lumped to distributed via semi-distributed: Calibration strategies for semi-distributed hydrologic models, J. Hydrol., 418, 61–77, 2012.
 - Laipelt, L., De Paiva, R. C. D., Fan, F. M., Collischonn, W., Papa, F., and Ruhoff, A.: SWOT Reveals How the 2024 Disastrous Flood in South Brazil Was Intensified by Increased Water Slope and Wind Forcing, Geophys. Res. Lett., 52, e2024GL111287, https://doi.org/10.1029/2024GL111287, 2025.
- Landuyt, L., Van Wesemael, A., Schumann, G. J.-P., Hostache, R., Verhoest, N. E., and Van Coillie, F. M.: Flood mapping based on synthetic aperture radar: An assessment of established approaches, IEEE Trans. Geosci. Remote Sens., 57, 722–739, 2018.
 - Li, H., Zhang, J., Cai, X., Huang, H., and Wang, L.: On the capacity of ICESat-2 laser altimetry for river level retrieval: An investigation in the Ohio River basin, J. Hydrol., 626, 130277, 2023.
- Marquis, G., Paradis, A., and Bonnier-Roy, F.: Étude hydrogéomorphologique et recommandations concernant la problématique d'inondation et de mobilité de la rivière des Mares à Baie-Saint-Paul, Avizo Experts-Conseils, Québec, Canada, 2024.





- Station 051305: https://www.cehq.gouv.qc.ca/hydrometrie/historique_donnees/fiche_station.asp?NoStation=051305, last access: 12 November 2025.
- 470 Mishra, A. K. and Coulibaly, P.: Developments in hydrometric network design: A review, Rev. Geophys., 47, 2007RG000243, https://doi.org/10.1029/2007RG000243, 2009.
 - Moghim, S., Gharehtoragh, M. A., and Safaie, A.: Performance of the flood models in different topographies, J. Hydrol., 620, 129446, 2023.
- Nair, A. S., Soman, M. K., Girish, P., Karmakar, S., and Indu, J.: Evaluating SWOT water level information using a large scale hydrology simulator: A case study over India, Adv. Space Res., 70, 1362–1374, 2022.
 - Nielsen, K., Zakharova, E., Tarpanelli, A., Andersen, O. B., and Benveniste, J.: River levels from multi mission altimetry, a statistical approach, Remote Sens. Environ., 270, 112876, 2022.
 - Patidar, G., Indu, J., and Karmakar, S.: Performance Assessment of Surface Water and Ocean Topography (SWOT) Mission for WSE Measurement Across India, Geophys. Res. Lett., 52, e2025GL115804, https://doi.org/10.1029/2025GL115804, 2025.
- 480 Station 03057: https://www.marees.gc.ca/fr/stations/03057/2023-05-14?tz=EDT&unit=m, last access: 12 November 2025.
 - Peral, E., Esteban-Fernández, D., Rodríguez, E., McWatters, D., De Bleser, J.-W., Ahmed, R., Chen, A. C., Slimko, E., Somawardhana, R., and Knarr, K.: KaRIn, the Ka-band radar interferometer of the SWOT mission: Design and in-flight performance, IEEE Trans. Geosci. Remote Sens., 62, 1–27, 2024.
- Schneider, R., Tarpanelli, A., Nielsen, K., Madsen, H., and Bauer-Gottwein, P.: Evaluation of multi-mode CryoSat-2 altimetry data over the Po River against in situ data and a hydrodynamic model, Adv. Water Resour., 112, 17–26, 2018.
 - Shen, Y., Liu, D., Jiang, L., Yin, J., Nielsen, K., Bauer-Gottwein, P., Guo, S., and Wang, J.: On the contribution of satellite altimetry-derived water surface elevation to hydrodynamic model calibration in the han river, Remote Sens., 12, 4087, 2020.
- Stuurman, C., Pottier, C., Chen, C., Fjortoft, R., Pavelsky, T., and Crétaux, J.-F.: Surface Water and Ocean Topography Project
 Algorithm Theoretical Basis Document. Level 2 KaRIn High Rate River Single Pass Science Algorithm Software, Jet
 Propulsion Laboratory (JPL), California Institute of Technology, and CNES, Pasadena, California, USA / Toulouse, France,
 2023.
 - Stuurman, C., Claire, P., Roger, F., Curtis, C., Stirling, A., and Lionel, Z.: SWOT Product Description: Level 2 KaRIn High Rate River Single Pass Vector Product, Pasadena, California, USA / Toulouse, France, 2025.
- Teng, J., Jakeman, A. J., Vaze, J., Croke, B. F., Dutta, D., and Kim, S.: Flood inundation modelling: A review of methods, recent advances and uncertainty analysis, Environ. Model. Softw., 90, 201–216, 2017.
 - Wood, M., Hostache, R., Neal, J., Wagener, T., Giustarini, L., Chini, M., Corato, G., Matgen, P., and Bates, P.: Calibration of channel depth and friction parameters in the LISFLOOD-FP hydraulic model using medium-resolution SAR data and identifiability techniques, Hydrol. Earth Syst. Sci., 20, 4983–4997, 2016.
- Yu, L., Zhang, H., Gong, W., and Ma, X.: Validation of mainland water level elevation products from SWOT satellite, IEEE J. Sel. Top. Appl. Earth Obs. Remote Sens., 17, 13494–13505, 2024.





Zhou, H., Liu, S., Mo, X., Hu, S., Zhang, L., Ma, J., Bandini, F., Grosen, H., and Bauer-Gottwein, P.: Calibrating a hydrodynamic model using water surface elevation determined from ICESat-2 derived cross-section and Sentinel-2 retrieved sub-pixel river width, Remote Sens. Environ., 298, 113796, 2023.